31st Annual International Conference of the IEEE EMBS
Minneapolis, Minnesota, USA, September 2-6, 2009

Precision of Syndesmophyte Volume Measurement for Ankylosing Spondylitis: a Phantom Study Using High Resolution CT

Sovira Tan, Jianhua Yao, Lawrence Yao, and Michael M. Ward

Abstract— **Ankylosing Spondylitis is a disease characterized by abnormal bone structures (syndesmophytes) growing at intervertebral disk spaces (IDS). The growth of syndesmophytes is typically monitored by visual inspection of radiographs. The limitations inherent to the modality (2D projection of a 3D object) and rater (qualitative human judgment) entail a possibly important loss in sensitivity. We previously presented a method designed to overcome both limitations: a computer algorithm that quantitatively measures syndesmophytes in the 3D space of a high-resolution computed tomography scan. To establish the method's usefulness for longitudinal studies, it is necessary to assess its precision (repeatability) which can be affected by the limitations of both the algorithm itself and the imaging modality. To this end, an anthropomorphic vertebral phantom with syndesmophytes in 4 IDSs was manufactured. It was scanned 22 times with varying positions and resolutions. The syndesmophyte volumes extracted by our algorithm have an average coefficient of variation of 1.6% per IDS and 0.85% for the total.**

I. Introduction

ANKYLOSING Spondylitis is a relatively rare inflammatory disorder that affects the spine and joints. It can be characterized by abnormal bone structures (syndesmophytes) growing at inter-vertebral disk spaces, which may lead to spinal rigidity and eventual spinal fusion [1]. Recently, while new drugs have been shown to considerably reduce signs of inflammation, it remains unclear if this is accompanied by a reduction in syndesmophyte formation [2],[3]. However, the growth of syndesmophytes has traditionally been monitored by visual inspection of plain radiographs. This is the case in [2] and [3]. The limitations inherent to the modality (2D projection of a 3D object) and rater (qualitative human judgment) entail a possibly important loss in sensitivity. We previously presented a method designed to overcome both limitations: a computer algorithm that quantitatively measures syndesmophytes in the 3D space of a high-resolution computed tomography scan. In a cross-sectional study the method was found to correlate well with a physician's rating [4]. However, to establish the method's usefulness in a longitudinal study, it is necessary to assess its precision (repeatability). That is the purpose of the present paper.

Ideally the same syndesmophyte scanned at different times should yield the same volume. Unfortunately variability is introduced by the limitations of scanner performance and those of the algorithm. Quantifying this variability is crucial in order to determine what can reliably be considered true change. Because of the harmfulness of X-rays, we specifically designed and manufactured an anthropomorphic vertebral phantom for repeated scanning. For this study it was scanned 22 times in varying positions and resolutions. The syndesmophytes volumes extracted by our algorithm were analyzed to quantify their variability.

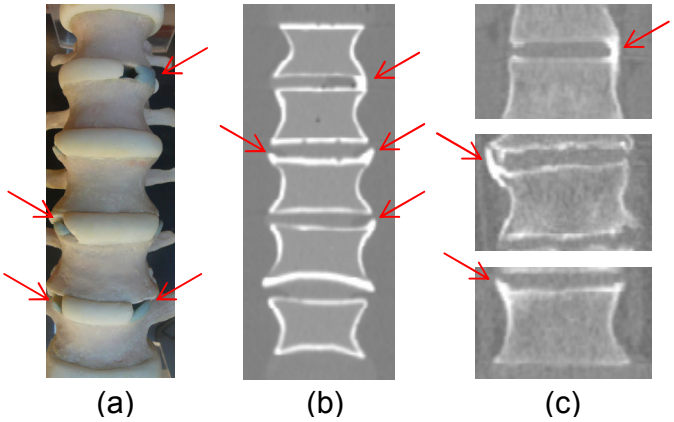

Fig. 1. Syndesmophytes (arrows) on (a) a photograph of the phantom (b) a scan of the phantom (c) scans of real patients.

II. Materials and Methods

A. Spine phantom and scanning protocol

The phantom was manufactured by CIRS (Norfolk, VA). It consists of 5 anthropomorphic vertebral bodies forming 4 IDSs. Both cortical and trabecular bone are made of epoxy resin, although of different densities (respectively 1200mg/cc in a soft tissue matrix and 250mg/cc of calcium hydroxyapatite in a marrow equivalent matrix). Syndesmophytes are made of cortical bone. One IDS has a bridging syndesmophyte, the 3 others each have 2 non-bridging syndesmophytes. The phantom is contained in an acrylic tank. The tank was filled with water to mimic surrounding soft tissue. Fig. 1(a) shows a photographic view of the phantom, Fig. 1(b) a coronal slice of the phantom's scan where 4 syndesmophytes are visible (the top one is the bridging syndesmophyte). For comparison Fig. 1(c) shows real syndesmophytes.

Manuscript received April 22, 2009. This research was supported by the Intramural Research Program of the NIH, NIAMS and CC.

S. Tan and M. M. Ward are with the National Institute of Arthritis and Musculoskeletal and Skin diseases, National Institutes of Health, Clinical Center, 10 Center Drive MSC 1182, Bethesda, MD 20892 USA (e-mail: tanso@ mail.nih.gov).

J. Yao, and L. Yao are with the Department of Diagnostic Radiology, National Institutes of Health, Clinical Center, Bethesda, MD 20892 USA.

The phantom was scanned on a Philips Brilliance 64 (64-detector row). Scanning parameters were 120 kVp, 300 mAs/slice, 1.5 mm slice thickness. For the reconstruction, kernel C (sharp) was used, spacing between slices was 0.7 mm. Two different reconstruction diameters (RD) were used, 40 and 46 cm. Those parameters are representative of those used for real patients. Two series were made, reconstructed respectively with RD 40 and 46 cm. RD 46 results in an image with lower resolution compared with RD 40. Each series has 11 scans. Between each scan the phantom was slightly rotated by about 1 degree. Fig. 2 shows scans corresponding to the extreme angles. There is 10 degree difference between the two. The reasons for moving the phantom between scans are: 1) CT scanner artifacts such as beam hardening can be dependent on positioning. 2) Our computer vision algorithm can also be affected by varying positions.

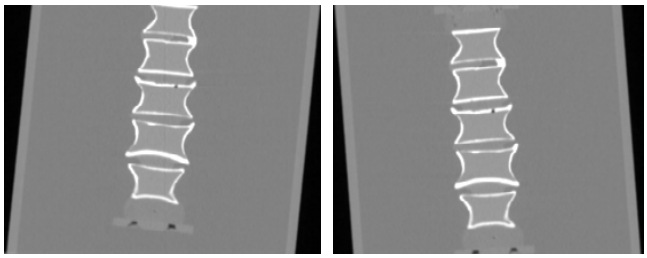

Fig. 2. Scans at extreme angle positions. The orientation difference between the scans is about 10 degrees.

B. Computer aided syndesmophyte volume extraction

Our original method for syndesmophyte segmentation was described in [4]. It is visually summarized in Fig. 3. First the whole vertebral body is segmented using a 3D multi-scale, multi-stage level set method. A triangular mesh representation of the segmentation is obtained using the Marching Cubes algorithm. It is this mesh that is visualized in Fig. 3. Then the endplates and ridgelines are extracted using another level set evolving on the mesh representation of the vertebral surface. This level set is guided by curvature features. Finally syndesmophytes can be cut from the vertebral body using the local ridgeline as the 0 level.

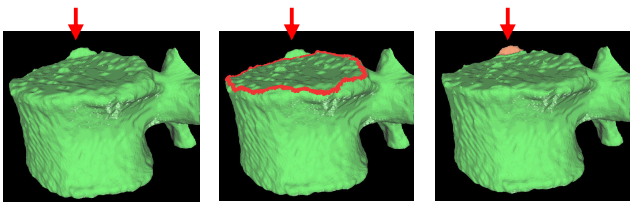

(a) (b) (c)

Fig. 3. Overview of the original syndesmophyte segmentation method. (a) Segmentation of the vertebral body (b) Detection of the end plate's ridgeline (c) Segmentation of the syndesmophyte. This figure is from Ref. 4.

However, that algorithm was only designed for a cross-sectional study. For a longitudinal study, where high precision is required, several important modifications were needed:

1) Syndesmophytes must be cut relative to the same ridgeline level. However different scans of the same vertebra will not be identical and the results of the ridgeline extraction will also differ. To ensure that no variation comes from inconsistencies between ridgelines we only use one reference ridgeline for all the scans. In the present work, that reference ridgeline comes from the scan at mid orientation angle between the extremes shown in Fig. 2 and reconstructed with RD 40. However, to be able to use the same ridgeline for 2 scans in different positions, those must be registered. We perform that registration using a landmark-based iterative closest point (ICP) algorithm [5]. Fig. 4 shows an IDS with the vertebral bodies corresponding to an extreme orientation angle scan (green) registered to those of the reference scan (red). The ridgeline of the reference scan (yellow) was used to cut the syndesmophytes for both scans. The syndesmophytes are pictured in bright colors to distinguish them from vertebral bodies (dark colors).

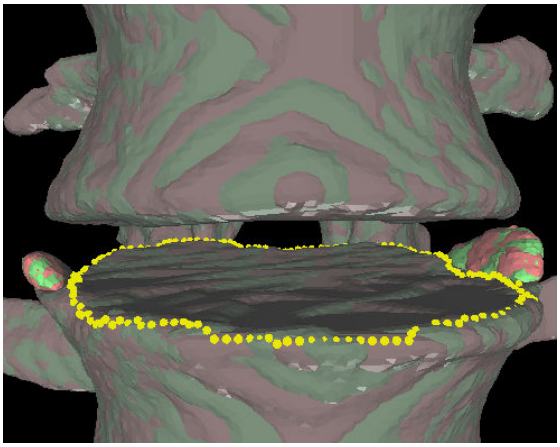

Fig. 4. Cutting of syndesmophytes from registered vertebral bodies relative to a reference ridgeline (yellow). Syndesmophytes and vertebral bodies are shown respectively in bright and dark colors.

2) At the boundary between bone and water, the representation of a continuous space by discrete voxels introduces the well-known partial volume effect, as some voxels contain both bone and water. Depending on the position of the syndesmophyte relative to the discrete grid, voxel intensity at the boundary will vary and a binary segmentation will arbitrarily include or leave out partial voxels, which will affect the precision of volume measurement. We devised a method for incorporating all partial voxels, assigning them a partial volume value depending on their grey level intensity.

At the end of the initial syndesmophyte segmentation, voxels are labeled as syndesmophyte, vertebral body or water. Using this initial segmentation, we mark voxels as interior syndesmophyte (S_i), boundary syndesmophyte (S_b), first water layer (W_1) and second water layer (W_2). S_b voxels are syndesmophyte voxels with at least one water neighbor.

S_i voxels are syndesmophyte voxels with no water neighbor. The first water layer is defined as water voxels with at least one syndesmophyte neighbor. The second water layer is made of water voxels with at least one W_1 neighbor but no syndesmophyte neighbor. S_b and W_1 voxels are the most affected by partial volume affect. We therefore use S_i voxels and W_2 voxels to respectively estimate the mean voxel intensity for syndesmophyte, GL_S, and for water, GL_W. We then use GL_S and GL_W to assign a partial syndesmophyte content to S_b and W_1 voxels. Let V be a S_b or W_1 voxel, and GL its grey level intensity. If GL is smaller than GL_W then it is classified as a water voxel. If it is larger than GL_S it is classified as syndesmophyte. If it is in between, we estimate its partial syndesmophyte volume as:

$$PSV = \frac{GL - GL_W}{GL_S - GL_W} \cdot p_x \cdot p_y \cdot p_z \qquad (1)$$

where p_x, p_y and p_z are the pixel sizes. Fig. 5 shows an axial slice of the bridging syndesmophyte. Fig. 5-(a) shows the initial binary segmentation and Fig. 5-(b) the segmentation with partial volume effect taken into account for S_b and W_1 voxels. The color red denotes complete syndesmophyte voxels. The colors magenta, yellow, green and blue respectively denotes partial syndesmophyte content of [100% to 75%], [75% to 50%], [50% to 25%] and [25% to 0%].

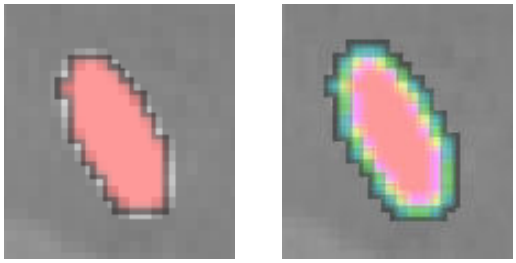

(a) (b)

Fig. 5. Axial slice of the bridging syndesmophyte. (a) Initial binary segmentation. (b) Color coded for partial volume effect (the code is explained in the text).

3) In a similar way, the representation of a continuous space by discrete voxels can also introduce inaccuracies in the syndesmophyte cutting algorithm. In our previous work a whole voxel was considered either above or below the local ridgeline level. However, in reality, most voxels close to the ridgeline level are neither completely above nor completely below that level. Rather, part of the voxel is above while the other part is below. In the present work we introduce a refinement in the syndesmophyte cutting algorithm in order to achieve subvoxel accuracy. First we extract the normal to the end plate, $\vec{N}$, using a least square estimate method [4]. Let V be a voxel under consideration. We determine the local ridgeline level in the following way. The ridgeline point closest to V is found. Neighboring ridgeline and endplate points are averaged to form the point R_V, which, as an average, is an estimate more robust to noise. R_V and $\vec{N}$ define a plane P, that can be used to cut syndesmophyte from vertebral body. We now determine the position of V relative to this plane. V is a rectangle defined by 8 vertices V_i with i $\in \{1,\ldots,8\}$. The sign of the scalar product:

$$s(V_i) = sign(\overrightarrow{R_V V_i} \cdot \vec{N}) \qquad (2)$$

tells us if V_i is above or below the plane P. If all signs are positive or negative, then voxel V is either completely a syndesmophyte voxel or not. If we have a mix, then V is a partial syndesmophyte voxel. To determine what proportion of V is syndesmophyte, we subdivide V into smaller rectangles. The locations of the vertices of the new subvoxels are $\left(i \cdot \frac{p_x}{M}, j \cdot \frac{p_y}{M}, k \cdot \frac{p_z}{M} \right)$ where p_x, p_y and p_z are the original pixel sizes, (i, j, k) are integers and M is the number of subdivisions. Here we chose M=10, which means each voxel is divided into 1000 subvoxels. Then, for each subvoxel, it is straightforward to determine if it is above or below P using the same scalar product (Equation 2). However, since we do not want to pursue the subdivision process further, it is not necessary to test all 8 vertices. We only test one, corresponding to the smallest (i, j, k). Let N_S be the number of subvoxels of V found to be syndesmophyte. Its corresponding partial syndesmophyte volume is:

$$PSV = \frac{N_S}{M^3} \cdot p_x \cdot p_y \cdot p_z \qquad (3)$$

After partial voxels (in respect to both bone/water and ridgeline boundaries) have been determined, it is straightforward to compute syndesmophyte volumes by adding complete voxels and partial voxels.

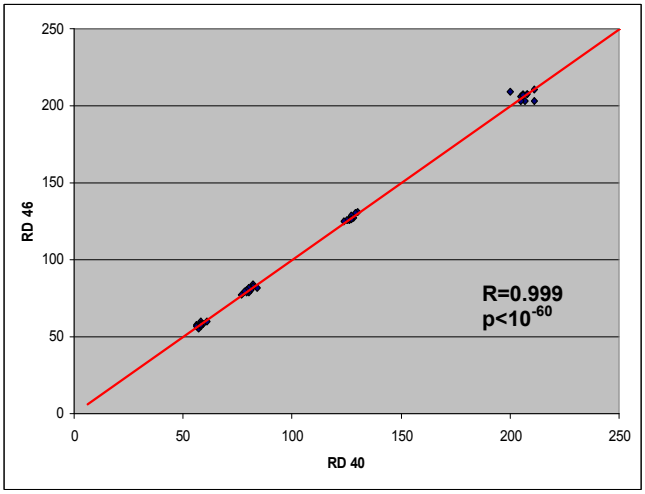

Fig. 6. Correlation between volumes obtained with RD 40 and RD 46.

III. Experimental Results

The volumes obtained using the method described above are statistically analyzed to quantify the precision of syndesmophyte measurements. We first examine the effects of the 2 reconstruction resolutions. In Fig. 6 we plot the measures (in mm^3) obtained with RD 40 versus those obtained with RD 46. Each point corresponds to the syndesmophyte volume in one IDS and at one orientation angle. There are 4 IDSs and 11 angles. The number of points is therefore 44. The correlation coefficient is 0.999 ($p<10^{-60}$). For each point we compute the fractional difference defined as the absolute difference between the RD 40 and RD 46 volume estimates divided by the mean of those estimates. The mean and standard deviation of this fractional difference are respectively 0.0118 and 0.0101. This experiment suggests that the two resolutions chosen for reconstruction do not result in large differences in the syndesmophyte volumes extracted by the algorithm.

We then investigate the variability that results from changing the position of the phantom. Table I shows the standard deviations, means and coefficients of variation (CV) for the two series of 11 angles. The coefficient of variation is defined as the standard deviation divided by the mean. The unit for standard deviation and mean is mm^3. We report volumes per IDS and total volume. Results for the 2 resolutions are similar. CV values range between 1.21% and 2.38%. For both series, the CV for total syndesmophyte volume is around 1%. This figure is lower than any CV per IDS. This fact suggests that compensation between errors might occur across IDSs, making total syndesmophyte volume a possibly more robust measure.

TABLE I
COEFFICIENTS OF VARIATION FOR VARYING POSITIONS

		IDS1	IDS2	IDS3	IDS4	TOTAL
RD 40	std	2.90	1.60	1.91	1.35	4.19
	mean	207	127	80.3	58	472
	CV	1.40%	1.26%	2.38%	2.33%	0.89%
RD 46	std	2.50	1.67	1.78	1.16	4.99
	mean	207	128	80.5	58.1	473
	CV	1.21%	1.30%	2.21%	2.00%	1.06%

Finally we want to provide an estimate of the total variability that results from all factors combined. We therefore merge the two sets corresponding to the two reconstruction resolutions and extract the new CV values, which we list in Table II (R40-a). The average CV per IDS is 1.77%. The CV for the whole phantom is still around 1%. We also investigate if the choice of a specific reference ridgeline affects the precision of the volume measurements. The one used so far is named R40-a. We repeat the experiment with 3 other ridgelines, corresponding respectively to RD 46-medium angle (R46-a), RD 40-extreme angle (R40-b) and RD 46-extreme angle (R46-b). The extreme angle is the one on the right of Fig. 2. The results for the 4 ridgelines are presented in Table II. Each value is for all the 22 scans. Note that the mean volumes are different. Different scans produce different ridgelines that cut syndesmophytes at different levels. That is why using one ridgeline is important for longitudinal studies. The results in Table II show that the choice of a reference ridgeline does not affect precision. All 4 ridgelines yield similar CV values. The average CVs per IDS are respectively 1.77%, 1.64%, 1.47% and 1.61%. CVs for the whole phantom vary from 0.8% to 0.98%. If we average the CVs for the 4 ridgelines we obtain an overall CV of 1.62% per IDS and 0.85% per total.

TABLE II
COEFFICIENTS OF VARIATION FOR DIFFERENT REFERENCE RIDGELINES (RESOLUTION GROUPS ARE MERGED)

		IDS1	IDS2	IDS3	IDS4	TOTAL
R40-a	std	2.71	1.66	1.85	1.26	4.63
	mean	207	127	80.4	58	472
	CV	1.31%	1.31%	2.30%	2.17%	0.98%
R46-a	std	2.73	1.78	1.64	0.9	3.65
	mean	195	127	78.4	53.5	453
	CV	1.40%	1.40%	2.09%	1.68%	0.81%
R40-b	std	2.56	1.92	1.21	1.26	4.02
	mean	221	133	73.1	78.1	505
	CV	1.16%	1.44%	1.66%	1.61%	0.80%
R46-b	std	2.41	2.08	1.55	1.22	3.89
	mean	197	131	84	68	481
	CV	1.22%	1.59%	1.85%	1.79%	0.81%

IV. Conclusion

In our previous work [4] we presented what was the first computerized method to quantitate syndesmophyte volumes in the full 3D space rather than on 2D radiographs. The method was validated in a cross-sectional study. In view of a longitudinal study, we have now investigated the precision of this algorithm using an anthropomorphic vertebral phantom. We scanned that phantom 22 times in varying positions and at 2 reconstruction resolutions. The coefficients of variation obtained were 1.62% per IDS and 0.85% for the whole phantom. Those results are promising for future work with clinical data.

References

[1] Arnett F.C., Ankylosing spondylitis, In: Koopman WJ, ed. Arthritis and Allied Conditions. 13 ed. Baltimore: Williams and Wilkins, pp. 1197-1208, 1997.

[2] Van der Heidjde, D., Landewe R., Einstein S., et al., "Radiographic progression of Ankylosing Spondylitis after up to two years of treatment with Etanercept", Arthritis & Rheumatism 58, pp. 1324-1331, 2008.

[3] Van der Heidjde, D., Landewe R., Baraliakos X., et al., "Radiographic findings following two years of Infliximab therapy with patients with Ankylosing Spondylitis", Arthritis & Rheumatism 58, pp. 3063-3970, 2008.

[4] Tan S., Yao J., Ward M.M., et al., "Computer aided evaluation of Ankylosing Spondylitis using high resolution CT", IEEE Trans. on Medical Imaging 27, pp. 1252-1267, 2008.

[5] Tan S., Yao J., Yao L., Summers R.M., Ward M.M., "Vertebral surface registration using ridgelines/crestlines", Proc. SPIE Medical Imaging 6914, San Diego, California, 69140H, 2008.